K-space thermodynamic funneling of light via heat exchange

Zhongfei Xiong,[1] Fan O. Wu,[2] Jing-Tao Lü,[3] Zhichao Ruan,[4] Demetrios N. Christodoulides,[2] and Yuntian Chen[1,5,*]

[1]*School of Optical and Electronic Information, Huazhong University of Science and Technology, Wuhan 430074, China*
[2]*CREOL, The College of Optics and Photonics, University of Central Florida, Orlando, Florida 32816-2700, USA*
[3]*School of Physics, Huazhong University of Science and Technology, Wuhan 430074, China*
[4]*Physics Department, Zhejiang University, Hangzhou, 310027, China*
[5]*Wuhan National Laboratory for Optoelectronics, Huazhong University of Science and Technology, Wuhan 430074, China*

(Received 24 October 2021; accepted 2 March 2022; published 31 March 2022)

We provide a thermodynamic approach to channel light into a single mode, i.e., the fundamental mode or the highest-order mode in the nonlinear multimode optical systems, via Rayleigh-Jeans condensation on both sides of the optical spectrum. Essentially, such *K*-space light funneling is driven by the effective thermodynamics force, i.e., the gradient of effective temperature or effective chemical potential, which can be manipulated through heat exchange via an external optical thermodynamic system. In a sandwich structure of optical nonlinear waveguide lattices, the temperature gradient between two subsystems with orthogonal polarization of light gives rise to the heat diffusion through an intermediate layer with cross-phase modulation, which cools down or warms up one of subsystems approaching zero temperature. Even though 100% funneling rate is unattainable as bounded by the third law of thermodynamics, we show that more than 90% occupation rate of fundamental mode or highest-order mode can be achieved via supercooling or superheating in this sandwich structure.

DOI: 10.1103/PhysRevA.105.033529

I. INTRODUCTION

In weak nonlinear regime, *K*-space funneling of light into lowest- or highest-order mode has a deep connection to optical thermodynamics [1–6], which was developed very recently and provides an alternative yet interesting playground for probing fundamental issues in thermodynamics. In application-orientated scenarios, *K*-space funneling of light might be useful in the construction of an all-optical Ising machine, where the ground state can be approximately reached during the thermalization process, instead of complicated optoelectronic feedback in a spatial optical Ising machine [7–10] and photonic recurrent Ising sampler [11,12], or suffering scaling limitation due to dispersion and decoherence in coherent Ising machines [13–17].

Recent works [18,19] reported Rayleigh-Jeans (R-J) condensation, a classical counterpart of Bose-Einstein condensation (BEC) in multimode optical systems, where the singularity occurs as the effective chemical potential reaches the lowest or highest-energy level. Notably, such photon-photon interaction-induced condensation is largely different from BEC of photons [20–25] and exciton-polaritons [26,27] in quantum systems, where the temperature is essentially dictated by the thermal bath or environment. Inspired by those findings, we find R-J condensation can occur at both sides of the optical spectrum by properly tuning the spectrum of input light to the nonlinear waveguide lattice. Consequently, *K*-space thermodynamic funneling of light into the highest or lowest-order mode can be realized, regardless of the detailed arrangement of the waveguide, as well as nonlinear hopping of the light among the normal modes. Furthermore, we can heat or cool a system to induce *K*-space light funneling by heat exchanging in a sandwich structure.

II. SCHEME

From the optical thermodynamics theory, the normalized power distribution of modes at equilibrium in highly multimode optical systems with weak nonlinearity is R-J distribution $|c_i|^2 = -T/(\varepsilon_i + \mu)$ [1–3,6], where c_i and ε_i are the amplitude and effective energy of the ith mode, respectively. Accordingly [1,2], the effective temperature T and effective chemical potential μ can been well defined ("effective" is omitted for simplicity onwards). As illustrated in Fig. 1, the optical temperature of the system can be changed by a nearby auxiliary optical system, which extracts (injects) "internal energy" from (into) the main system via heat conduction. As such, the optical thermodynamics force induced by the temperature gradient of the main optical system essentially drives the power flow funneled into the target mode in *K* space.

Specifically, the nonlinear optical system considered here is a nonlinear waveguide lattice [i.e., the inset in Fig. 2(a)], where each site contains self-phase modulation (SPM) that normally exists in nonlinear optical crystals, waveguides, and cavities. The rationale behind the thermodynamic funneling can be understood from R-J distribution of the nonlinear optical system at equilibrium. Essentially, the parameters T and μ in R-J distribution reveal the condition of the equilibrated nonlinear multimode system. Under the conserved total normalized power $P = \sum_{i=1}^{M} -T/(\varepsilon_i + \mu)$ (M is the mode

*yuntian@hust.edu.cn

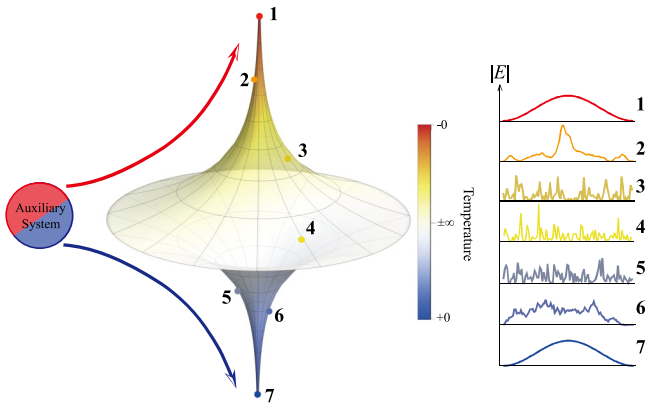

FIG. 1. Thermodynamics funneling of light in optical complex system with highly multimoded nonlinear wave interaction. The color coding indicates the temperature of the optical thermodynamical system. The contour lines denote the macroscopic states under the same temperature with exactly identical modal distribution $\{|c_i|^2\}$ yet different phases. With a suitable auxiliary system in contact, the system can be cooled down (warmed up in negative temperature) towards zero temperature; most of the optical power will be funneled into the lowest- (or highest-) order mode, indicated by the solid blue (red) circle, which will be narrowed down to a single point at zero temperature (lowest- and highest-order modes have same intensity profile but different phase in adjacent sites). By conducting with a suitable auxiliary system, cooled down or warmed up this system towards zero temperature is available.

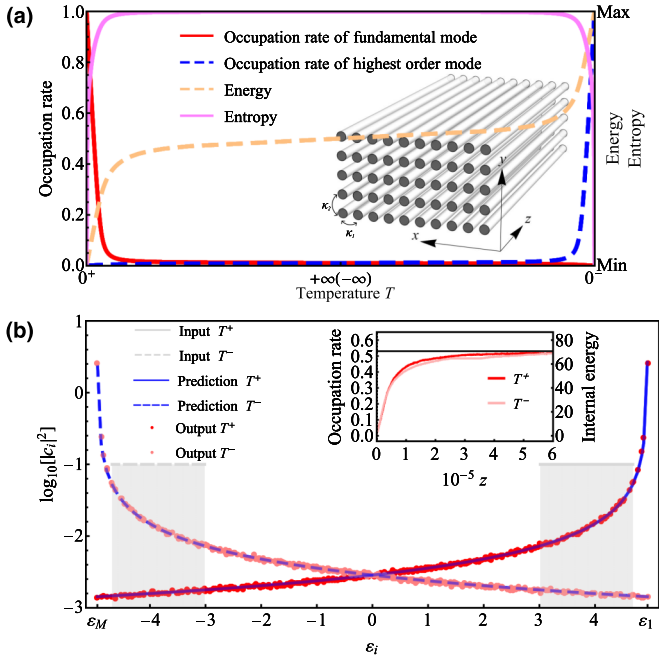

FIG. 2. (a) Temperature dependence of the occupation rate [the lowest-order mode in red (dark-gray) line, highest-order mode in blue (dark-gray) dashed line], internal energy [orange (light-gray) dashed line], and entropy [purple (light-gray) line] in a nonlinear waveguide lattice. Inset shows the schematic diagram of optical waveguide lattice with propagating direction along z axis, and the normalized linear coupling coefficients between waveguides are denoted by κ_1 in x direction and κ_2 in y direction, respectively. (b) Condensation in lowest- (highest-) order mode. The initial modal distribution launched into the waveguide lattice is indicated by light-gray rectangle region; red (dark-gray) and pink (light-gray) points show R-J distributions at thermal equilibrium. Blue solid (dashed) lines (dark-gray lines) show the predicted R-J distributions. The inset shows the variation of fundamental- [red (light-gray) line)] and highest-order [blue (dark-gray) line] mode occupation. All the simulation results are the average of 1000 ensemble copies; all the quantities are normalized and dimensionless.

number of system), the normalized internal energy (which accounts for the momentum flow) $U = \sum_{i=1}^{M} \varepsilon_i T/(\varepsilon_i + \mu) \in [-\varepsilon_1 P, -\varepsilon_M P]$ increases from $T = 0^+$ to 0^- as shown in Fig. 2(a), where $T = \pm\infty$ is the transition point. The difference between positive and negative temperature regime is the power occupation rate among the eigenmodes, i.e., the lower-order modes dominate in the positive temperature region while larger occupation rate of higher-order modes leads to negative temperature [28–33]. At $T = \pm\infty$, the occupation rates of all modes are the same. In contrast, at $T = 0$, the system condenses into the ground state or highest-order state, where entropy $S = \sum_{i=1}^{M} \ln |c_i|^2$ (defined in Ref. [1]) reaches minimal value.

III. CONDENSATION

Similar to BEC, as μ goes to the lowest-energy level $(-\varepsilon_1)$, the temperature T tends to 0^+ and U reaches its minimal value, which leads to a singular value in R-J distribution and has profound consequences. Indeed, the optical nonlinearity drives the optical system to condensate in the ground state [18]. By the same token, as μ approaches the highest-energy level $(-\varepsilon_M)$, T tends to 0^- and U reaches its maximal value, where the R-J distribution also has a singularity and consequently the optical system condensates in the highest-order mode [19].

The macroscopic occupancy, i.e., the power distribution $\{|c_i|^2\}$, as a function of the spectrum $\{\varepsilon_i\}$ on either side of the spectrum, is shown in Fig. 2(b). We study a rectangular lattice with 20×20 waveguides with normalized linear coupling $\kappa_1 = 1$ and $\kappa_2 = 1.5$. Two types of initial input field with rectangular line-shape function (solid and dashed light-gray lines, normalized input power $P = 5$ and input internal energy $U = \mp 19.12$) are launched. Evidently, in the initial condition, the portion of supermodes where the optical power is in the lowest- (highest)-order mode are negligible. As the light beam propagates, the nonlinear hopping of the optical power among the supermodes occurs and drives the optical system into thermal equilibrium, wherein the equilibrium temperature is $T^{\pm} = \pm 0.0141$, chemical potential is $\mu = -1.001\varepsilon_{1/M}$ as predicted from R-J distribution [1–3]. Condensation occurs in the fundamental (highest-order) mode as the lower- (higher-) order modes dominate. As evident from the inset of Fig. 2(b), the power of the lowest- (highest-)order mode increases from zero to 53%.

Despite that the thermalization process can be seen as a K-space funneling process at low temperature, it is difficult to achieve high funneling rate due to two reasons. Firstly, the final occupation rate is fixed by the internal energy and total power of the initial incidence, since the power distribution

$\{|c_i|^2\}$ obeys the R-J distribution that is merely determined by the initial condition. Secondly, the input condition with low equilibrated temperature by itself requires the input power concentrated on the lower modes, which in turn hinders the extra power funneling to fundamental mode. Such dilemma can be overcome by introducing an auxiliary system, which is contact with the main system to provide thermodynamic force that drives power flux in the main system flowing to target mode sets.

IV. THERMODYNAMIC FUNNELING

Conceptually, the occupation of the lowest- (highest-) order mode rises as the absolute value of the temperature decreases, as evident from Fig. 2(a). We consider two nonlinear waveguide lattices with completely orthogonal polarization, where the first system is coupled to the second optical system via an interlayer. As shown in Fig. 3(a), the two subsystems

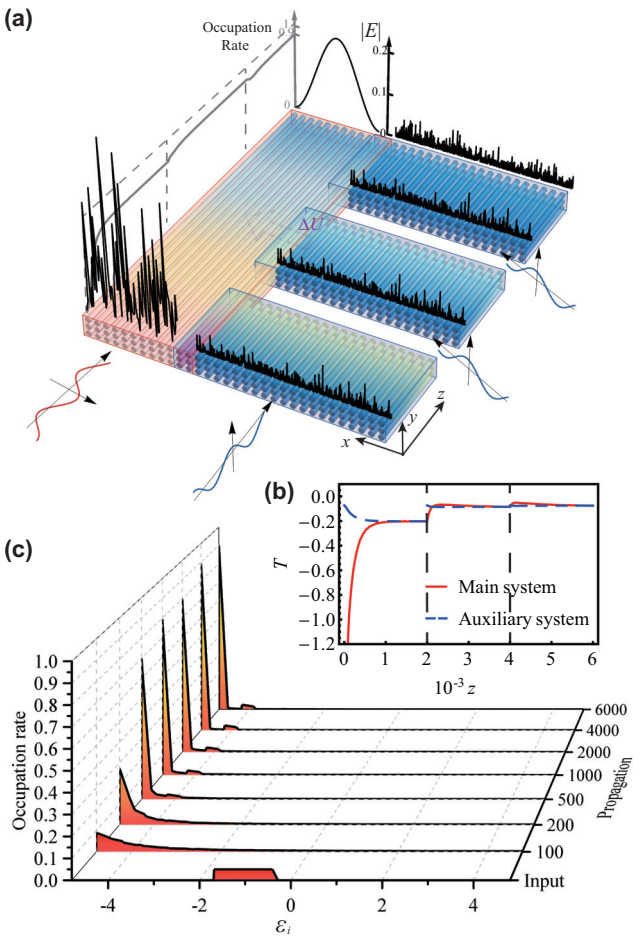

FIG. 3. *K*-space thermodynamic funneling of light by superheating. (a) Sketch of heat exchanging in a canonical ensemble system. Black lines indicate the spatial distribution of optical power. (b) The variation of equilibrium temperatures in left (red) and right (blue dashed) systems. (c) The evolution of modal occupation rate for target system as the light beam propagates along z axis. At $z = 6000$, more than 90% optical power is funneled into the highest-order mode.

are indicated by the red and blue boxes, in which either horizontal or vertical polarization is supported by properly adjusting the waveguide cross section. The interlayer indicated by the purple waveguides in the middle supports both two polarizations. In the presence of the cross-phase modulation (XPM), two subsystems are coupled together via the interlayer with exchanged internal energy but conserved power, thereby forming a rigorous canonical ensemble system [1]. Accordingly, even though the large differences between the subsystems, i.e., waveguides number, spectrum, and input power, may exist, the two subsystems shall have the same temperature as the whole system tends to equilibrium. In the presence of the temperature gradient between two waveguide lattices, the heat flow streams from the higher-temperature side to the lower side. As for the negative temperature, the heat flows from negative temperature to positive temperature since the negative temperature is hotter than positive temperature, i.e., $T \to 0^-$ is the hottest temperature [2]. Therefore, the well-designed auxiliary (right) subsystem can be used to heat up or cool down the main (left) systems via heat conduction. Consequently, by times heat conduction [we call it superheating (-cooling)], the temperature of the left subsystem can be approximately decreased to zero, wherein the singular behavior of the R-J distribution occurs and the significant funneling of optical power into the lowest- (highest-) order mode can be observed. As illustrated in Fig. 3(a), black lines represent the electric fields. After several iterations, the main subsystem condensates as output black line closing to lowest- (highest-) order mode, implying that the optical power distributed chaotically over the spectrum $\{\varepsilon_i\}$ at $z = 0$ is eventually funneled into the lowest- (highest-) order mode; thereby, the thermodynamically funneling is achieved as the gray line raises over 90%. Since the heat flow between two subsystems is only forced by temperature gradient rather than the occupation rate of modes, we can avoid using one already condensed subsystem to condense another one by designing the parameters of the auxiliary subsystem; black lines are chaotic in the right subsystem in Fig. 3(a), implying the lowest- (highest-) order mode keeps a very low occupation rate.

We illustrate the idea of thermodynamically funneling of optical power to the highest-order mode via superheating the main system that is close to negative temperature condensation in Fig. 3. The left (right) waveguide lattice is 10×10 (10×120), the normalized linear coupling between waveguides are both $\kappa_1 = 1$ and $\kappa_2 = 1.5$, the normalized input power is 40 (80), and the ensemble copies is 1000. As for the main system, the temperature of the input state is $T_{1in} = -2.41$, with $T_1 = -0.11$ for 90% occupation of highest mode, while the temperature in equilibrium of the auxiliary lattice is around $T_{2in} = -0.073$ with $T_2 = -0.0074$ for 90% occupation. After three iterations, i.e., $z = 6000$, the temperature of the main subsystem is increased to $T_{1\text{end}} = -0.076$ as shown in Fig. 3(a). Remarkably, more than 90% optical power is thermodynamically funneled into the highest-order mode, as evident in Fig. 3(c). The temperature and the occupation rate in highest-order mode in the main system are $(-0.1971, -0.0831, -0.0740)$ and $(82.36\%, 92.53\%, 93.24\%)$ by optical thermodynamic theory [1], in comparison with numerically simulated values being $(-0.2041, -0.0854, -0.0760)$

and (80%, 89.31%, 90.07%), as the heat exchange is finished in the three iterations. The theoretical prediction is a bit larger than real simulation results due to the assumption that the total internal energy is conserved, which does not hold exactly and part of the internal energy is converted into nonlinear counterpart as discussed shortly. Notably, after two iterations with $z = 4000$, the occupation rate exceeds 90%, as shown in Fig. 3(c). Further increasing the occupation rate of the target mode requires more iterations and longer equilibrium time (not shown here), which diverge as the temperature approaches absolute zero. The rationale behind this is the third law of thermodynamics, which leads to the fact that the condensation into absolute-zero temperature is impossible in a finite number of steps [34,35] and thus the unitary thermodynamic funneling of light into the highest- or lowest-order mode is unattainable. Nevertheless, without any parameter optimization, we show that more than 90% optical power can be thermodynamically funneled into the target mode in our simple setting via heat exchange.

V. DISCUSSION

The condensation phenomenon does not necessarily occur in the nonlinear waveguide lattice system due to the existence of modulation instability (MI) and the generation of the spatial soliton for larger input power [36]. The optical thermodynamics theory only admits low-input optical power, where the internal energy, i.e., the linear part of total Hamiltonian $U = -H_L$, is approximately conserved. Otherwise, the nonlinear part H_{NL} dominates, and the spatial soliton might appear [36]. The precursor of spatial soliton is MI, which depends on the balance between nonlinearity [represented by γ in Eq. (1)] and diffraction coefficient [$D(k_x) = d^2\beta/dk_x^2$] [36]. According to the band dispersion, there are two types of dispersion regions: (1) $D < 0$ (normal diffraction) at low-order modes, and (2) $D > 0$ (anomalous diffraction) at high-order modes. Most of the photonic waveguide system has a focusing Kerr nonlinearity ($\gamma > 0$); the thermodynamic funneling into ground state fails due to the MI condition ($D\gamma < 0$) for mode group with normal diffraction being satisfied such that the change of nonlinear Hamiltonian is not negligible. Instead, the thermodynamic funneling into the highest mode which bears anomalous diffraction still works. If the optical system has a defocusing nonlinearity, i.e., $\gamma < 0$, the thermodynamic funneling works for fundamental mode but fails for highest-order mode, as summarized in Fig. 4(a).

Indeed, Fig. 4(b) shows the light propagation in the nonlinear coupled waveguide lattice with the identical settings as that in Fig. 2, except that the normalized input power is increased to 20. The z-dependent occupation rate of highest mode (solid pink line) increases from zero to 0.53 (black line), overlapped exactly with the prediction from optical thermodynamic theory. In contrast, the final occupation rate of the ground state (solid red line) is less than 2%, where the prediction from R-J distribution fails. In addition, the internal energy in the negative temperature regime (pink dashed line) with $\gamma D > 0$ is conserved during the propagation. In sharp contrast, the internal energy in positive temperature regime (red dashed line) with $\gamma D < 0$ decreases as light beam propagates, due to the transfer of internal energy to the nonlinear

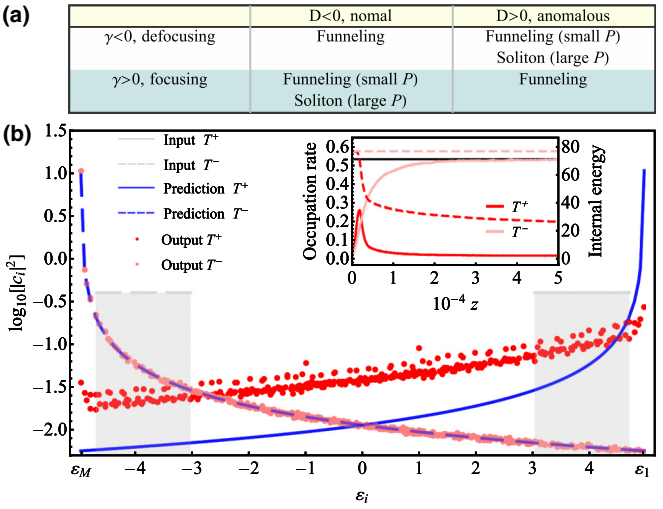

FIG. 4. Funneling and soliton formation in the lowest- and highest-order modes, respectively. (a) The funneling condition with the sign of nonlinearity γ and the sign of diffusion D. (b) Input and output power distributions with P increasing to 20 for the same system in Fig. 2 ($\gamma > 0$). All the simulation results are the averaged results of 1000 ensembles. Inset: Occupation rates (lines) and absolute internal energy (dashed lines) along the propagation.

Hamiltonian, which is confirmed by the space soliton formation at the lattice center in each ensemble copy in the full simulation. Therefore, in this typically chosen scenario shown in Fig. 4(b), the condensation to highest-order mode still exists the same as Fig. 2(b), evidenced by the excellent agreement of the ε_i-dependent power distribution between the prediction from optical thermodynamic theory (the blue-dashed line) and the full simulations (pink dots). As for the ground state, the prediction from R-J distribution (blue line) fails due to the internal energy not being conserved; thus, optical thermodynamic theory is not applicable.

VI. CONCLUSION

In conclusion, we proposed an optical thermodynamically approach to funnel light into single mode in a nonlinear multimode optical system. The nonlinear optical waveguide lattice has a finite spectrum, featuring two different types of condensation on the two sides of the spectrum, which are used to realize the thermodynamic funneling of light into the lowest- and highest-order mode via heat conduction. Considering the thermal isolation of the nonlinear waveguide lattice, we use a sandwich structure with two orthometric polarization to realize the heat exchange without changing the optical power. Importantly, with properly designed auxiliary waveguide lattice, any optical waveguide lattice can be cooled down or heated up such that the optical power is funneled to the fundamental- or highest-order mode, up to 90% if the MI and the spatial soliton formation can be well suppressed.

As an outlook, our work of realizing the thermodynamic funneling into the highest-order mode explicitly reveals the possibility of negative temperature condensation, which indicates that an optical thermodynamic system provides an alternative yet interesting playground to address fundamental

issues in thermodynamics and quantum thermodynamics. In addition, our work might be useful in realizing an all-optical Ising machine in nonlinear photonic pseudospin systems like nonlinear ring resonator lattice [37] or spatial photonic Ising machine [7–10], where the ground state might be approached simply by a pure heat-exchanging process rather than hybrid feedback with complicated algorithms.

ACKNOWLEDGMENTS

This work is supported by National Natural Science Foundation of China (NSFC) Grants No. 11874026, No. 21873033, No. 91850108, and No. 12174340, the program for the HUST academic frontier youth team, ONR MURI (Grant No. N00014-20-1-2789), AFOSR MURI (Grants No. FA9550-20-1-0322 and No. FA9550-21-1-0202), National Science Foundation (Grants No. DMR-1420620 and No. EECS-1711230), Simons Collaboration (Simons Grant No. 733682), W.M. Keck Foundation, U.S.-Israel Binational Science Foundation (Grant No. 2016381), U.S. Air Force Research Laboratory (Grant No. FA86511820019), and the Qatar National Research Fund (Grant No. NPRP13S0121-200126).

APPENDIX

In a (2+1)-dimensional rectangular waveguide lattice [the inset in Fig. 2(a)], the normalized nonlinear Schrödinger equation (NSE) can be written as [1,2]

$$i\frac{da_{m,n}}{dz} + \kappa_1(a_{m-1,n} + a_{m+1,n}) + \kappa_2(a_{m,n-1} + a_{m,n+1}) + \gamma|a_{m,n}|^2 a_{m,n} = 0, \tag{A1}$$

where $a_{m,n}$ is the amplitude of optical modal field in the single-mode waveguide indexed by two subscripts m and n along the x and y direction, respectively; κ_1 and κ_2 are coupling constants in the x and y direction, respectively; γ describes the strength of self-phase modulation in each waveguide; and z is normalized propagating distance. The linear part of the waveguide lattice (the linear Hamiltonian H_L) is characterized by linear spectrum, i.e., a series of waveguide supermodes with propagation constants β_i ($\{\beta_1 > \beta_2 > \cdots > 0 > \cdots > \beta_{M-1} > \beta_M\}$). By defining effective energy $\varepsilon_i = \beta_i$, then the optical ground state has the largest energy level while the highest-order state has the smallest energy level. The total power $P = \sum_{i=1}^{M} |c_i|^2$ and total Hamiltonian $H = H_L + H_{NL}$ (H_{NL} represents nonlinear part of Hamiltonian) are two conserved quantities, where c_i ($|c_i|^2$) is the amplitude (power) of the ith supermode. Since the nonlinearity is weak, $H_L \gg H_{NL}$, relative momentum flow $U = -H_L = \sum_{i=1}^{M} -\varepsilon_i|c_i|^2$ can be seen as an approximate conserved internal energy. The total power P and momentum flow U (coined as the internal energy onwards) play identical roles as the particle number and internal energy in thermodynamics, where the optical nonlinearity irreversibly drives the optical system towards the equilibrium state with the highest entropy during light propagation [1]. In equilibrium, one could find the power distribution (particle occupation distribution) on the supermode spectrum is an R-J distribution, $|c_i|^2 = -T/(\varepsilon_i + \mu)$ [1–3].

For the sandwich lattice in Fig. 3(a), the NSE for the sites on the left (red) or right (blue) lattice is just Eq. (A1), but we need to add an XPM term in the NSE for the sites in the interlayer lattice (purple):

$$i\frac{da_{m,n}}{dz} + \kappa_1(a_{m-1,n} + a_{m+1,n}) + \kappa_2(a_{m,n-1} + a_{m,n+1}) + \gamma_{SPM}\,|a_{m,n}|^2 a_{m,n} + \gamma_{XPM}|b_{m,n}|^2 a_{m,n} = 0, \tag{A2}$$

where $b_{m,n}$ is the amplitude of another polarization at site (m, n); γ_{SPM} and γ_{XPM} are the strength of SPM and XPM, respectively.

Given the initial temperature and internal energy of two subsystems, one can predict the final temperature of two subsystems with heat capacity. For a regular 1D lattice, an approximation heat capacity is $C_M(T) = M - |T|M^2(T^2M^2 + 4\kappa^2P^2)^{-1/2}$ [4]. For 2D lattice, there is no explicit formulation of heat capacity, but we could use a numerical heat capacity from $U = \sum_{i=1}^{M} \varepsilon_i T/(\varepsilon_i + (U - TM)/P)$ and use a graphical way of predicting the final temperature [1]. For instance, the total energy of total systems $U_0 = U_1 + U_2$ (where U_1 and U_2 are the energy of two subsystems) is assumed as a conserved quantity, we draw the curve $T_1(U_1)$ and curve $T_2(U_2) = T_2(U_0 - U_1)$, and find the crossing point $T(U_1)$ as the final temperature.

[1] F. O. Wu, A. U. Hassan, and D. N. Christodoulides, Thermodynamic theory of highly multimoded nonlinear optical systems, Nat. Photonics **13**, 776 (2019).

[2] M. Parto, F. O. Wu, P. S. Jung, K. Makris, and D. N. Christodoulides, Thermodynamic conditions governing the optical temperature and chemical potential in nonlinear highly multimoded photonic systems, Opt. Lett. **44**, 3936 (2019).

[3] K. G. Makris, F. O. Wu, P. S. Jung, and D. N. Christodoulides, Statistical mechanics of weakly nonlinear optical multimode gases, Opt. Lett. **45**, 1651 (2020).

[4] F. O. Wu, P. S. Jung, M. Parto, M. Khajavikhan, and D. N. Christodoulides, Entropic thermodynamics of nonlinear photonic chain networks, Commun. Phys. **3**, 216 (2020).

[5] N. K. Efremidis and D. N. Christodoulides, Fundamental entropic processes in the theory of optical thermodynamics, Phys. Rev. A **103**, 043517 (2021).

[6] A. Ramos, L. Fernández-Alcázar, T. Kottos, and B. Shapiro, Optical Phase Transitions in Photonic Networks: A Spin-System Formulation, Phys. Rev. X **10**, 031024 (2020).

[7] D. Pierangeli, G. Marcucci, and C. Conti, Large-Scale Photonic Ising Machine by Spatial Light Modulation, Phys. Rev. Lett. **122**, 213902 (2019).

[8] D. Pierangeli, G. Marcucci, and C. Conti, Adiabatic evolution on a spatial-photonic Ising machine, Optica **7**, 1535 (2020).

[9] D. Pierangeli, G. Marcucci, D. Brunner, and C. Conti, Noise-enhanced spatial-photonic Ising machine, Nanophotonics **9**, 4109 (2020).

[10] Y. Fang, J. Huang, and Z. Ruan, Experimental Observation of Phase Transitions in Spatial Photonic Ising Machine, Phys. Rev. Lett. **127**, 043902 (2021); J. Huang, Y. Fang, and Z. Ruan, Antiferromagnetic spatial photonic Ising machine through optoelectronic correlation computing, Commun. Phys. **4**, 242 (2021).

[11] M. Prabhu, C. Roques-Carmes, Y. Shen, N. Harris, L. Jing, J. Carolan, R. Hamerly, T. Baehr-Jones, M. Hochberg, V. Čeperić *et al.*, Accelerating recurrent Ising machines in photonic integrated circuits, Optica **7**, 551 (2020).

[12] C. Roques-Carmes, Y. Shen, C. Zanoci, M. Prabhu, F. Atieh, L. Jing, T. Dubček, C. Mao, M. R. Johnson, V. Čeperić *et al.*, Heuristic recurrent algorithms for photonic Ising machines, Nat. Commun. **11**, 249 (2020).

[13] A. Marandi, Z. Wang, K. Takata, R. L. Byer, and Y. Yamamoto, Network of time-multiplexed optical parametric oscillators as a coherent Ising machine, Nat. Photonic **8**, 937 (2014).

[14] T. Inagaki, K. Inaba, R. Hamerly, K. Inoue, Y. Yamamoto, and H. Takesue, Large-scale Ising spin network based on degenerate optical parametric oscillators, Nat. Photonics **10**, 415 (2016).

[15] P. L. McMahon, A. Marandi, Y. Haribara, R. Hamerly, C. Langrock, S. Tamate, T. Inagaki, H. Takesue, S. Utsunomiya, K. Aihara *et al.*, A fully programmable 100-spin coherent Ising machine with all-to-all connections, Science **354**, 614 (2016).

[16] T. Inagaki, Y. Haribara, K. Igarashi, T. Sonobe, S. Tamate, T. Honjo, A. Marandi, P. L. McMahon, T. Umeki, K. Enbutsu *et al.*, A coherent Ising machine for 2000-node optimization problems, Science **354**, 603 (2016).

[17] Q. Cen, T. Hap, H. Ding, S. Guan, Z. Qin, K. Xu, Y. Dai, and M. Li, Microwave photonic Ising machine, arXiv:2011.00064.

[18] K. Baudin, A. Fusaro, K. Krupa, J. Garnier, S. Rica, G. Millot, and A. Picozzi, Classical Rayleigh-Jeans Condensation of Light Waves: Observation and Thermodynamic Characterization, Phys. Rev. Lett. **125**, 244101 (2020).

[19] K. Baudin, A. Fusaro, J. Garnier, N. Berti, K. Krupa, I. Carusotto, S. Rica, G. Millot, and A. Picozzi, Energy and wave-action flows underlying Rayleigh-Jeans thermalization of optical waves propagating in a multimode fiber (a), EPL (Europhysics Letters) **134**, 14001 (2021).

[20] J. Klaers, J. Schimitt, F. Vewinger, and M. Weitz, Bose–Einstein condensation of photons in an optical microcavity, Nature (London) **468**, 545 (2010).

[21] C. Sun, S. Jia, C. Barsi, S. Rica, A. Picozzi, and J. W. Fleischer, Observation of the kinetic condensation of classical waves, Nat. Phys. **8**, 470 (2012).

[22] D. Dung, C. Kurtscheid, T. Damm, J. Schmitt, F. Vewinger, M. Weitz, and J. Klaer, Variable potentials for thermalized light and coupled condensates, Nat. Photonics **11**, 565 (2017).

[23] B. Walker, L. C. Flatten, H. J. Hesten, F. Mintert, D. Hunger, A. A. Trichet, J. M. Smith, and R. A. Nyman, Driven-dissipative non-equilibrium Bose–Einstein condensation of less than ten photons, Nat. Phys. **14**, 1173 (2018).

[24] R. Weill, A. Bekker, B. Levit, and B. Fischer, Bose–Einstein condensation of photons in an Erbium–Ytterbium co-doped fiber cavity, Nat. Commun. **10**, 747 (2019).

[25] C. Kurtscheid, D. Dung, E. Busley, F. Vewinger, A. Rosch, and M. Weitz, Thermally condensing photons into a coherently split state of light, Science **366**, 894 (2019).

[26] T. Byrnes, N. Y. Kim, and Y. Yamamoto, Exciton–polariton condensates, Nat. Phys. **10**, 803 (2014).

[27] R. Su, S. Ghosh, J. Wang, S. Liu, C. Diederichs, T. C. H. Liew, and Q. Xiong, Observation of exciton polariton condensation in a perovskite lattice at room temperature, Nat. Phys. **16**, 301 (2020).

[28] N. F. Ramsay, Thermodynamics and statistical mechanics at negative absolute temperatures, Phys. Rev. **103**, 20 (1956).

[29] P. T. Landsberg, Negative temperatures, J. Phys. A **10**, 1773 (1977).

[30] A. Rapp, S. Mandt, and A. Rosch, Equilibration Rates and Negative Absolute Temperatures for Ultracold Atoms in Optical Lattices, Phys. Rev. Lett. **105**, 220405 (2010).

[31] E. M. Purcell and R. V. Pound, A nuclear spin system at negative temperature, Phys. Rev. **81**, 279 (1951).

[32] P. Hakonen and O. V. Lounasmaa, Negative absolute temperatures: "Hot" spins in spontaneous magnetic order, Science **265**, 1821 (1994).

[33] S. Braun, J. P. Ronzheimer, M. Schreibar, S. S. Hodgman, T. Rom, I. Bloch, and U. Schnerder, Negative absolute temperature for motional degrees of freedom, Science **339**, 52 (2013).

[34] H. B. Callen, *Thermodynamics and an Introduction to Thermostatistics* (Wiley, New York, 1998).

[35] S. J. Blundell and K. M. Blundell, *Concepts in Thermal Physics*, (Oxford University Press, Oxford, 2009).

[36] F. Lederer, G. I. Stegeman, D. N. Christodoulides, G. Assanto, M. Segev, and Y. Silberberg, Discrete solitons in optics, Phys. Rep. **463**, 1 (2008).

[37] H. Yang, J. Xu, Z. Xiong, X. Lu, R.-Y. Zhang, H. Li, Y. Chen, and S. Zhang, Optically Reconfigurable Spin-Valley Hall Effect of Light in Coupled Nonlinear Ring Resonator Lattice, Phys. Rev. Lett. **127**, 043904(2021).